In Situ Characterization of Two Wireless Transmission Schemes for Ingestible Capsules

Lei Wang, *Member, IEEE*, Timothy D. Drysdale, and David R. S. Cumming*

***Abstract*—We report the experimental *in situ* characterization of 30–40 MHz and 868 MHz wireless transmission schemes for ingestible capsules, in porcine carcasses. This includes a detailed study of the performance of a magnetically coupled near-field very high-frequency (VHF) transmission scheme that requires only one eighth of the volume and one quarter of the power consumption of existing 868-MHz solutions. Our *in situ* measurements tested the performance of four different capsules specially constructed for this study (two variants of each transmission scheme), in two scenarios. One mimicked the performance of a body-worn receiving coil, while the other allowed the characterization of the direction-dependent signal attenuation due to losses in the surrounding tissue. We found that the magnetically coupled near-field VHF telemetry scheme presents an attractive option for future, miniturized ingestible capsules for medical applications.**

***Index Terms*—Biomedical telemetry, finite-difference time-domain (FDTD) methods, UHF radio propagation, VHF radio propagation.**

I. Introduction

THERE IS great interest in the use of wireless transmission systems in and around the body, for applications as diverse as medicine [1] and personal entertainment [2]. In diagnosis and screening of the gastrointestinal (GI) tract, self-contained wireless capsules with integrated sensors [3] offer significant benefits such as improved patient comfort and wider test coverage, in terms of both time and area. For example, ingestible capsules painlessly allow unprecedented ease of access to the entire GI tract, whereas conventional endoscopic examination leaves up to two thirds of the small bowel unexamined and is sufficiently uncomfortable to merit sedation [4].

The first examples of wireless medical capsules were developed beginning in the late 1950s and measured temperature [5], pressure [6], or pH [7]. Little further progress [8] was made until the recent development of a video capsule [4]. However, video is only one of the several measurements that physicians wish to obtain from the GI tract. Accurate measurements of temperature, pressure, pH and other ion concentrations can reveal pathologies that are undetectable by video. It is essential in many cases to obtain this information for the entire GI tract. Depending on GI motility, this can take up to 72 hours. Existing capsules with short lifetimes leave significant portions unexamined. The battery is limited in size by patient comfort constraints, so the power consumption must be reduced in order to improve capsule longevity [9]. The key problem is the large power consumed by the RF transmitter in overcoming the strong, frequency-dependent attenuation of the signal in the human body. In experimental work, Scanlon *et al.* [10] observed significant transmission loss of 19–25 dB at 915 MHz, using a vaginal implantable telemeter. A capsule in the GI tract is even deeper in the body, requiring the ability to transmit through up to 15 cm of human tissue. While the efficiency of a small antenna increases with frequency, so too does the attenuation of the tissue [11]. Taking both these effects into account, finite-difference time-domain (FDTD) simulations by Chirwa *et al.* [12] in the frequency range 150 MHz–1.2 GHz predicted that optimal transmission from a pill inside a human body was achieved at 600–800 MHz.

This range does not exactly correspond with the license-free industrial, scientific, and medical (ISM) bands that are available to these capsules (433 MHz, 868 MHz, and 2.4 GHz in Europe and 315 MHz, 915 MHz, and 2.4 GHz in the U.S.). Given that prototype capsules have already been developed with telemetry systems operating at these less-than-optimal frequency ranges [9], [13], [14] and above [15], there is clearly a need for an improved solution. Any such solution must be constructed from readily available, inexpensive components in order to meet the low-cost requirement for these one-time-only/disposable devices.

Following the success of near-field transmission schemes in radio-frequency identification applications [16], an attractive approach is to use magnetic induction (coupling) [17], and operate in the 300-kHz–30-MHz frequency band allocated to ingestible capsule devices by the Medicines and Healthcare products Regulatory Agency (MHRA) [18]. At these frequencies, the wavelength ($10\ \mathrm{m} < \lambda_0 < 1\ \mathrm{km}$) is much larger than the pill itself so it is impossible to incorporate a conventional antenna arrangement. Instead, an inductor (small coil) is employed as the radiating element. The inductor generates an alternating magnetic field around the pill, the amplitude of which falls with the cube of distance but will mutually couple to a receiving coil located in the near field ($\mathrm{r} < \lambda_0/2\pi$). To date, there has been no published performance comparison of the low-frequency near-field induction transmission technique with the previously studied far-field high-frequency techniques, for ingested capsule applications.

Manuscript received July 10, 2006; revised February 3, 2007. The work of T. D. Drysdale was supported by a Royal Society of Edinburgh Personal Research Fellowship. *Asterisk indicates corresponding author.*

L. Wang and T. D. Drysdale are with the Department of Electronics and Electrical Engineering, University of Glasgow, Glasgow G12 8LT, U.K. (e-mail: t.drysdale@elec.gla.ac.uk).

*D. R. S. Cumming is with the Department of Electronics and Electrical Engineering, University of Glasgow, Rankine Building, Oakfield Avenue, Glasgow G12 8LT, U.K. (e-mail: d.cumming@elec.gla.ac.uk).

The authors wish it to be known that, in their opinion, the first two authors should be regarded as joint First Authors.

Digital Object Identifier 10.1109/TBME.2007.895105

TABLE I
DETAILED SPECIFICATION OF THE FOUR CAPSULES CONSTRUCTED FOR THIS STUDY

	LF1	LF2	HF1	HF2
Carrier frequency (MHz)	32	40	868	868
Power consumption (mW@3V)	5	6	21	22
Operating distance in air (m)	< 0.5 [17]		>5	>5
Maximum data rate (kbps)	5		10	10
Radiator / antenna type	Coil inductor (Epcos B82498)		Helical (Linx JJB)	Patch (Linx Splatch)
Radiator / antenna dimensions (mm^3)	1 x 1 x 0.5		∅7 *l*9	27 x 13 x 1.5
Transmitter dimensions (mm^3)	8 x 5 x 3, coil embedded		20 x 10 x 2	20 x 10 x 2
Wireless device net volume (transmitter + antenna mm^3)	120		910	930
Capsule dimensions (mm^3) * includes batteries; others not	∅11 *l*35	∅15 *l*45 *	∅12 *l*40	∅15 *l*50

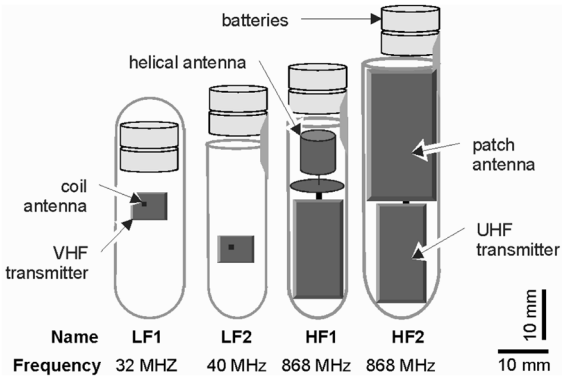

Fig. 1. Schematic diagrams of the four ingestible capsules studied in this paper showing the relative sizes of the radio frequency transmitter and antenna components. The biosensor- and system-on-a-chip components are not shown.

In this paper, we report the first implementation of the novel near-field magnetic coupling very high-frequency (VHF) telemetry scheme, and compare its measured *in situ* performance against similar capsules employing conventional ultrahigh-frequency (UHF) telemetry schemes. In Section II, we describe the construction of the capsules, their transmission schemes (32–40 MHz and 868 MHz), and the preparation of the porcine carcasses used for the *in situ* measurements. In Section III, we outline the procedure for measuring the *in situ* radiation patterns that are presented in Section IV. In Section V, we evaluate and compare the performance of the transmission schemes in terms of transmission loss and power consumption, showing the improved performance afforded by the novel near-field magnetic coupling scheme.

II. MATERIALS

Four different capsules were constructed for this study, as shown in the schematic diagram of Fig. 1. Each capsule contains sensors and circuits [19], a transmitter, and an antenna, is powered by two SR44 cells, and is packaged in a waterproof, nontoxic machined material (the 40-MHz capsule) or by potting in poly(dimethylsiloxane) (PDMS) (other capsules). The key difference between the capsules is the physical size and carrier frequency of the telemetry system. For further details of the capsules' construction, including a photograph, see [20].

Two of the capsules implemented the low-frequency inductive coupling method proposed in [17] at 32 and 40 MHz, respectively; we call these the "low-frequency" capsules: LF1 (32 MHz) and LF2 (40 MHz). The other two capsules implemented standard transmission schemes appropriate to the 868-MHz ISM band, but each used a different antenna; we call these the "high-frequency" capsules: HF1 and HF2. Table I lists the detailed specification of the four capsules.

In the high-frequency capsules, we deliberately used antennas that are among the smallest and most cost-effective of those commercially available for 868-MHz operation. Despite this, the volume of the ferrite-cored coil inductor [21] used as the antenna in the low-frequency capsules (LF1 and LF2) was only 1/700th of the volume of the helical antenna in HF1 and 1/1000th of the volume of the patch antenna in HF2. Considering the transmitter sizes as well, the low-frequency telemetry system occupied 1/8 of the volume and required 1/4 of the power compared to the 868-MHz systems. The low-frequency capsules LF1 and LF2 used a purpose-made FM transmitter and the inductor coil was mounted such that its longitudinal axis was aligned to the longitudinal axis of the capsule. The high-frequency capsules each contained the same 868-MHz commercial transmitter (FM-RTFQ from RFsolutions) and used a microstrip transmission line between the transmitter and antenna so as to minimize the RF signal loss [22]. HF1 also had a copper ground plane of area ca. 1 sq. cm below its helical antenna. For all four capsules, each transmitter had only a single communication channel and used frequency-shift keying (FSK) modulation.

A spectrum analyzer (HP4404 from Agilent) was used for RF signal reception, in conjunction with a receiving coil antenna. Two different home-made receive coils were constructed from copper wire and plastic formers: a large one (25-cm diameter, five turns) that fitted over the carcass and a small one (10-cm diameter, ten turns) that was pointed at the carcass. A BNC coaxial plug was attached to each coil, with one end of the coil attached to the signal line and the other end to ground. The larger coil could be easily worn by a human, omitting the plastic former for comfort and adjusting the coil diameter for fit. Without a former, the coil would conform to the contours of the subject's

body and, with a low-profile custom-built receive unit, could be worn under clothes without being noticed by others.

Other materials required for the experiments included an indoor motorized antenna rotator, stabilized laser line marker for alignment, affiliated plastic rotation stands and arms, and usual post-mortem equipment such as scalpels, stitches, and needles.

Fresh porcine carcasses were obtained from a nearby abattoir for use in the *in situ* measurements. The animals were 3–4 months old at expiration, and were slaughtered as part of routine commercial operation of the abattoir; they were not slaughtered specifically for our experiment. None of the carcasses had been bled out after slaughter. This was an advantage because we wanted the experimental conditions to mimic as closely as possible the conditions encountered in living tissue, where the presence of blood and other body fluids is expected to increase the overall conductivity and, therefore, reduce the transmissivity. The carcasses weighed approximately 25–35 kg.

III. Method

This section describes the measurement procedures for determining the direction-dependent transmission loss of the pills. The experiments were conducted in a large concrete post-mortem room of approximate dimension 7 m by 8 m with a 6-m high ceiling.

For the *in situ* measurements, the capsules were surgically embedded in porcine carcasses. Each capsule was measured in three different orientations: one vertical (with the *in situ* capsule parallel to the cranial–caudal line) and two horizontal (with the *in situ* capsule parallel to either the dorsal–ventral or lateral–medial line). The embedding procedure was as follows. With the carcass lying on an operation table, a midline incision was made along the abdomen from the xiphoid process of the sternum to the proximal inguinal teat, providing good access to the GI tract. For the dorsal–ventral (first horizontal) orientation, the capsule was inserted into a cut made to the diaphragm about 5 cm from the ventral attachment point. For the medial—lateral (second horizontal) orientation, the capsule was anchored by tying it to the intestinal mesentery. For the cranial–caudal (vertical) orientation, the capsule was inserted into the coils of the small intestine. In all three cases, the capsule was located within the abdomen between the T14 (thoracic) and L2 (lumbar) levels. After embedding the capsule, the incisions were sutured with nylon.

During the measurements, the carcass was hung by its forelegs from a metal hook and metal wire, with the head tied up with ordinary string to promote a vertical orientation of the spine. The low end of the carcass was approximately 1 m above the room ground. Two separate setups were used to obtain the measurements, as illustrated in the diagrams of Fig. 2, with the set-up for measuring the transverse directions in Fig. 2(a) and the azimuthal directions in Fig. 2(b). The transverse measurement mimics a body-worn receive coil, while the azimuthal measurements allow the direction-dependent transmission losses to be determined.

Transverse measurements were conducted on one horizontal (dorsal–ventral or lateral–medial) orientation only, due to time constraints, while azimuthal measurements were conducted for all three orientations. After each measurement was conducted, the orientation of the pill was rechecked by carefully reopening the incisions. The large antenna was placed completely around the carcass, with its longitudinal axis co-aligned with that of the carcass. The zero position was defined as the coil being centered upon the capsule location. Measurements were taken at 10-cm intervals while the coil was lowered, until the final measurement which was taken with the coil below the carcass, as illustrated in Fig. 2(a).

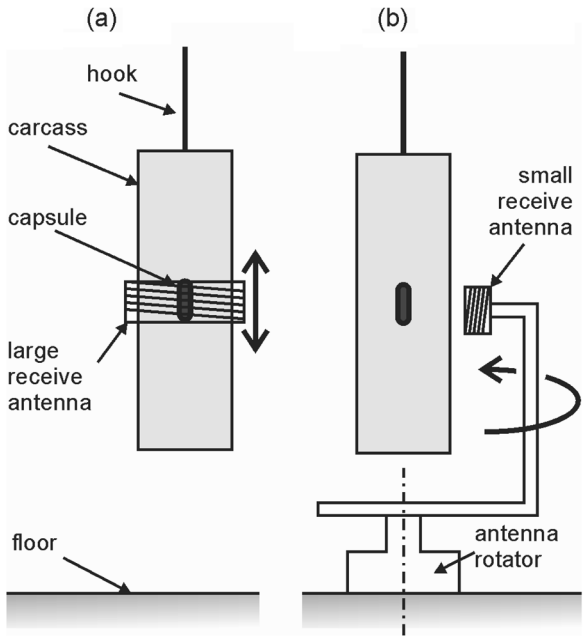

Fig. 2. Diagram of experimental set-up for *in situ* measurements. (a) Transverse measurement (large coil). (b) Azimuthal measurement (small coil). The size of the capsule is exaggerated for clarity.

The azimuthal measurements were taken with the small receive antenna, mounted upon the motorized antenna rotator via plastic support arms that were adjusted to obtain a small separation between the carcass and the front face of the antenna. This antenna scribed an arc of radius $r = 15$ cm around the capsule, yielding a separation from the carcass that varied from 1–3 cm because the cross section of the carcass was not round. Measurements were taken at angular steps of 30°, with 0° defined as being at the ventral incision point and the direction of positive rotation being ventral to lateral. The antenna was mounted so that it was oriented with its longitudinal axis normal to the surface of the carcass for all steps. Both clockwise and anticlockwise rotations were performed to eliminate hysteresis. In addition to the *in situ* measurements, the radiation pattern of the 32-MHz capsule LF1 was characterized by taking azimuthal measurements at heights of -40 cm to 40 cm in 10-cm steps. We do not present the radiation patterns of the helical and patch antennas here because they are well known in the literature [23].

For all measurements, the output of the receive coil was connected via coaxial cable to the spectrum analyzer, located 3 m away. All other objects were cleared from a 3-m radius around the experiment. The transmission loss (in dB) for any direction was calculated by subtracting the power (in dBm) received

when the capsule was embedded in the carcass (*in situ* measurement) from the power received in an identical setup but without the carcass present (control measurement). In order to correctly locate the capsule during the control measurements, a plastic stand was used. For each *in situ* and control measurement, the spectrum analyzer's frequency range was centred upon the capsule signal with a 100-kHz span and the RF noise floor readings were recorded. Each measurement was averaged 20 times.

Each capsule was powered by two 3-V SR44 battery cells. Battery lifetime tests conducted on each capsule indicated that the cells provide approximately 50 h effective lifetime for the low-frequency capsules and 12.5 h for the high-frequency capsules. For the sake of accurate characterization of *in situ* signal attenuation, the total measurement time span for all capsules was limited to much less than 12.5 h and the supply voltage was recorded before and after every measurement.

A full-vector numerical electromagnetic solver tool based on the FDTD method [24] was used to model the "in air" (control) and *in situ* radiation patterns of the antenna used in the low-frequency capsules LF1 and LF2. Small loop antennas have a radiation pattern that is independent of the exact geometry and can be accurately modelled with a single magnetic dipole [23]. The simulation domain for both simulations was a cube of 7.5 m in length per side, comprised of 320 by 320 by 320 cubic mesh cells. The domain was bounded by the perfectly matched layer condition, of 10 cells thickness on all sides. A single frequency source of 32 MHz with a raised cosine envelope excited a single magnetic field component at the centre of the domain. The simulations were run until convergence using a time step of 45 ps. The porcine carcass was represented by a cylinder of diameter 10 cells (23 cm) and height 36 cells (84 cm), having a complex refractive index of $n' = 12 - j8$. The refractive index was arbitrarily chosen to equal to the average of the individual refractive index values for various body tissue types at 32 MHz as presented in [25] because a detailed evaluation of the effective complex refractive index of the carcass was outside the scope of this paper. We note that there is no need to model the detailed structure of the carcass because its dimensions are small with respect to the wavelength.

IV. Results

The radiation patterns of the 32-MHz capsule LF1 in air are shown in Fig. 3, with the pill oriented vertically in Fig. 3(a) and horizontally in Fig. 3(b). The field patterns are cut away for clarity and a cylinder (not to scale) indicates the capsule orientation for clarity. These patterns correspond to those that are predicted by the equations in [17], when convolved with the receiving coil's radiation pattern. As expected for the vertically oriented capsule, there is a small trough (10 dB) at zero vertical displacement. Thus, it was decided to conduct the azimuthal *in situ* measurements for the vertically oriented low-frequency capsules at a vertical displacement of approximately 15 cm in order to obtain the strongest signal and hence highest quality characterization of any attenuation in the transmission path. The radiation pattern for the horizontal case in Fig. 3(b) differs from that in Fig. 3(a) because the relative orientations of

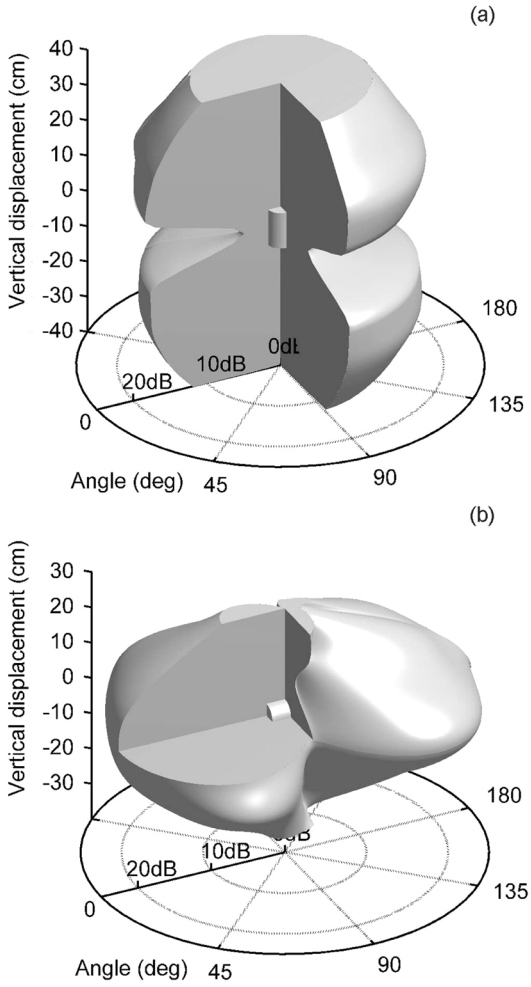

Fig. 3. Cylindrical coordinate plots of the measured radiation patterns of the LF1 low-frequency capsule (32 MHz) in air (control measurement), for (a) pill oriented vertically, and (b) pill oriented horizontally (axis lying along $0° - 180°$). The orientation of the pill is indicated by a cylinder (not to scale). The field patterns are partly cut away for clarity.

the transmit and receive antennas are different. Measurements of the horizontally oriented LF pills are, therefore, expected to obtain the greatest signal strength at a zero vertical displacement, as is known to be the case for the HF capsules.

The results obtained from the transverse measurement setup, designed to mimic a body-worn coil, are presented in Fig. 4. Both the low-frequency capsules (LF1 and LF2) gave their highest received powers (-84 and -89 dBm, respectively) when the receive coil was at or near the same height as the capsule. The received signal power reduced as the coil was moved further away from the capsules' position in the abdomen. This suggests that while acceptable received signal powers will be available for the coil located anywhere on the body, the optimum placement would be as close as possible to where the capsule will be when it is traversing the region of interest. The situation is similar for the high-frequency capsules HF1 and HF2, although the maximum received powers for these capsules were higher at -72 and -66 dBm, respectively. The slight offset in the position of the maximum received power is always less than 8 cm, and we attribute this to error in aligning

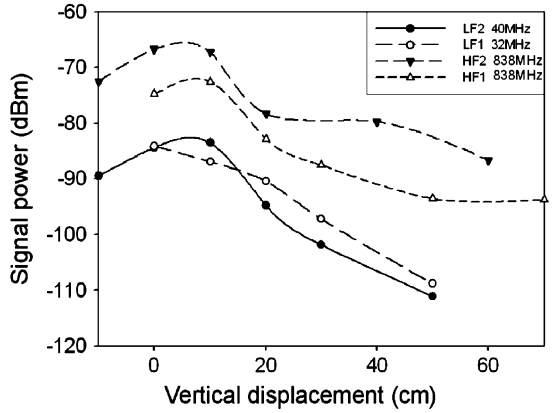

Fig. 4. Graph of the measured signal power as a function of the vertical displacement of the large receiving coil (transverse measurement, see Fig. 3(a) for each of the four capsules. In each case, the capsule is oriented horizontally.

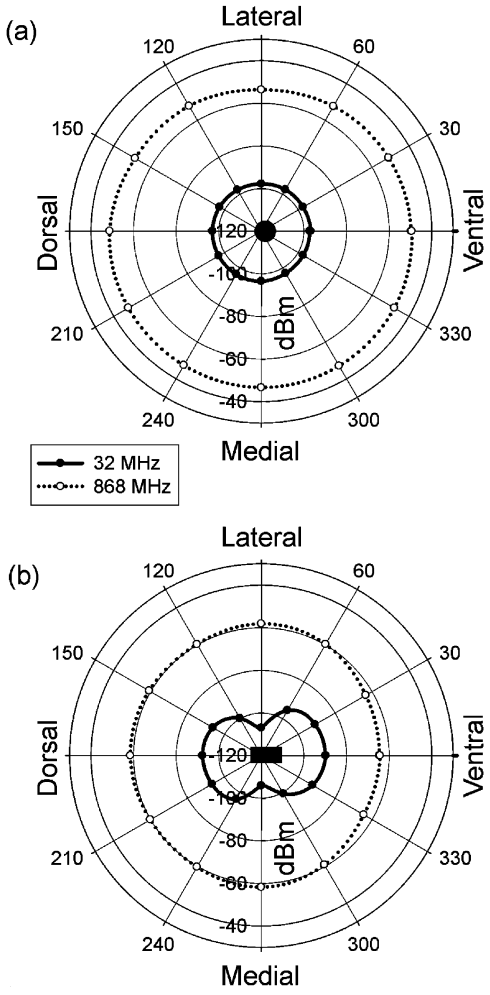

Fig. 5. Polar plots of control data for (a) the vertical and (b) the horizontal orientation of the capsules. Only one data set from each transmission scheme is shown: LF1 32 MHz with the solid line and HF1 868 MHz (JJB antenna) with the dotted line.

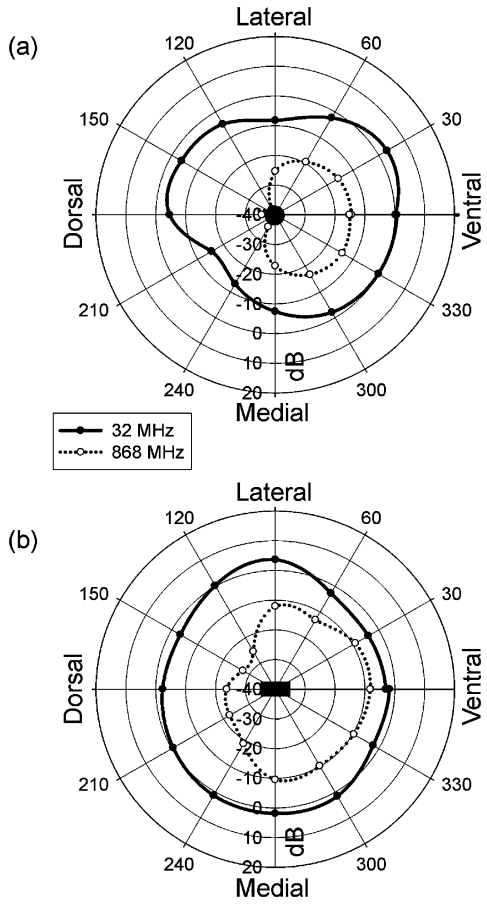

Fig. 6. Polar plots of the transmission of the embedded capsules (i.e., *in situ* measurement normalized against the control measurement) for (a) the vertical and (b) the horizontal orientation of the capsules. Only one data set from each transmission scheme is shown: LF1 32 MHz with the solid line and HF1 868 MHz (JJB antenna) with the dotted line.

the receive coil to the expected position of the capsule (± 3 cm) and the internal organs slumping when the carcass is hung, lowering the position of the capsule (≤ 5 cm). While the signal received from the HF capsules is approximately 17 dB stronger on average, this does not necessarily mean that the HF capsules represent a better solution as we will show later when we consider signal-to-noise ratios and relative power consumption.

The azimuthal measurements are intended to provide a direction-dependent characterization of the transmission loss in the carcass, defined as the difference between the received signal power when the capsule is in air and *in situ*. We present the control data first. Fig. 5 shows the received signal power recorded in the azimuthal control experiments, with the capsules oriented vertically in Fig. 5(a) and horizontally in Fig. 5(b). In the vertical orientation, the radiation is isotropic for both capsules with an average of -50 dBm received from capsule HF1 while an average of -97 dBm was received from capsule LF1. In the horizontal orientation, the radiation pattern from capsule HF1 remained isotropic, with similar averaged received power (-50 dBm). The radiation pattern of the low-frequency capsule LF1 exhibits the expected double lobe shape that was revealed in Fig. 3(b). On average, the received signal was -96 dBm, with the peaks of the lobes approximately 17 dB stronger than the troughs between them. In these control experiments conducted in air, the received signal powers for the high-frequency capsules were -65 dBm and -72 dBm, which were some 13–20 dB larger than that for the low-frequency capsules.

TABLE II
SUMMARY OF MEASUREMENT RESULTS

Capsule		Body-worn coil *in-situ*	Azimuth control		Azimuth *in-situ*			
	Noise Floor	Rec'd signal	Average rec'd signal		Aver age attenuation		Dorsal fading	
			Vert	Horiz	Vert	Horiz	Vert	Horiz
	dBm	dBm	dBm	dBm	dB	dB	dB	dB
LF1	-115±5	-84	-97	-96	5	1	0	0
LF2	-115±5	-89						
HF1	-90±5	-72	-50	-50	26	15	52	17
HF2	-90±5	-66						

Fig. 6 shows the direction dependent transmission loss (i.e., *in situ* data normalized to the control data of Fig. 5), with the capsules oriented vertically in Fig. 6(a) and horizontally in Fig. 6(b). In the vertical orientation, the 868-MHz capsule HF1 experiences strong attenuation of 26 dB on average, and there is significant channel fading of 52 dB in the dorsal direction that we attribute to stronger tissue absorption in that part of the carcass. Conversely, the 32-MHz capsule LF1 fares much better, experiencing attenuation of only 5 dB on average with no direction-dependent channel fading. In the horizontal orientation, both capsules perform better. The 868-MHz capsule exhibited 15 dB of attenuation on average and 17 dB of channel fading in the dorsal direction, while the 32-MHz capsule had very low attenuation of only 1 dB on average and a nearly omnidirectional antenna pattern. These measurement results are summarized in Table II.

We performed simulations that mimicked both the control and *in situ* azimuthal experiments for the case of the low-frequency capsule LF1. The simulation results were in good agreement with the measured results but we present only a selection for compactness. The simulated radiation pattern from a horizontally oriented 32-MHz capsule in air is shown in Fig. 7(a), corresponding to the measured control result in Fig. 5(b) that is drawn with the solid line. The simulated *in situ* transmission of a horizontally oriented 32-MHz capsule in shown in Fig. 7(b), and is normalized against the simulated control data from Fig. 7(a). The simulation data shown in Fig. 7(b) corresponds to the *in situ* measurement data plotted with the solid line in Fig. 6(b). Qualitatively, the simulated results in Fig. 7 agree well with the measured data in Figs. 5 and 6. We note that the magnitude of the simulated *in situ* radiation pattern is slightly enhanced overall by 1.2 dB compared to the simulated control radiation pattern because the carcass dielectric increases the effective electrical size and hence efficiency of the radiating element.

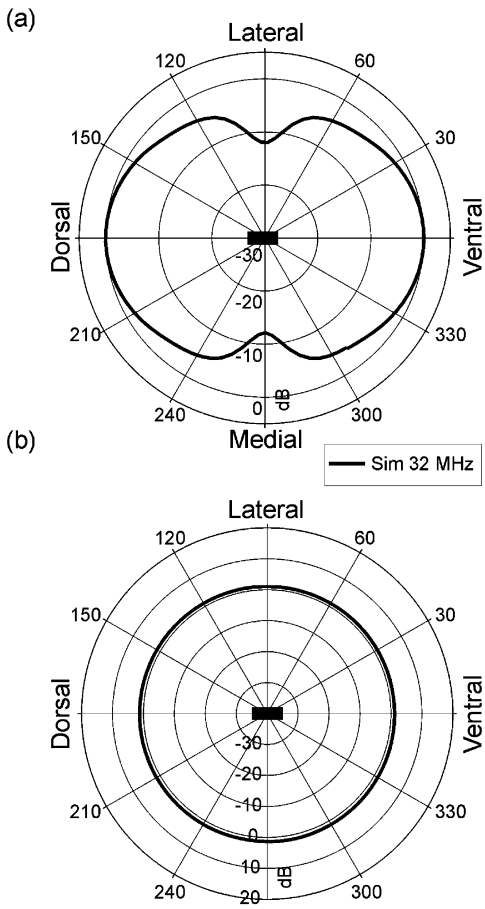

Fig. 7. Polar plots of simulated data at 32 MHz for the horizontally oriented capsule LF1: (a) control or radiation pattern, and (b) transmission of embedded capsule (i.e., *in situ* simulation normalized against control).

V. DISCUSSION

As expected, the magnetic near fields employed by the low-frequency transmission scheme are relatively unimpeded by the tissues, fluids, etc. in the carcass whereas the high-frequency far fields are strongly absorbed. For the 868-MHz scheme, the strong channel fading in the dorsal direction, as well as the generally lower level of signal received on the posterior side, is a consequence of the arrangement of organs, bone, fat, and blood within the carcass, each having different dielectric properties and absorption coefficients [12]. Thus, the low-frequency capsules have the advantage of avoiding data loss from channel fading. This is important because a capsule deployed in a live subject would be almost constantly in motion throughout the GI tract and also its orientation would be uncontrollable.

Furthermore, we estimate that the low-frequency capsules have the advantage of a better signal-to-noise ratio for a given level of power consumption, and, therefore, a higher quality signal. The measured power consumption figures indicate that the high-frequency capsules are transmitting at up to four times the power, or 6 dB stronger.

Subtracting the experimental noise floor (see Table II) from the HF capsules' average received signal powers in the *in situ* measurements gives a carrier signal-to-noise ratios (CSNRs) in the range of 11–16 dB depending on vertical/horizontal capsule orientation, whereas the LF capsules have a superior CSNR of 19 dB. This calculation is dependent upon the background noise where we conducted our measurements (-115 dBm for HF and -95 dBm for LF), but it also helps illustrate the advantage of using a near-field transmission scheme in an unlicensed band—nearby users contribute less to the background noise due to the $1/\mathrm{r}^3$ reduction in near-field strength compared to the $1/\mathrm{r}$ reduction associated with the propagating fields employed at 868 MHz.

Unfortunately for the 868-MHz transmitter, the data sheet indicates that its power consumption cannot be lowered below 20 mW, so the low-frequency transmission scheme that consumes only 5 mW (see Table I) is more attractive for long-lifetime capsules. The low-frequency scheme is inherently more power efficient because it takes advantage of the high amplitude of the near fields ($r = 15$ cm $\ll (\lambda_0/2\pi)$ at 32 MHz) compared to that of the propagating far fields ($r = 15$ cm $\gg (\lambda_0/2\pi)$ at 868 MHz).

VI. Conclusion

We constructed four ingestible capsules with the aim of comparing the performance of a novel near-field magnetically coupled transmission scheme for the 30-MHz ingestible capsule band against an existing commercial transmission scheme for the 868-MHz ISM band. We experimentally characterized the radiation pattern of the low-frequency antenna (a coil, operating at 32 MHz) in good agreement to theory, then conducted *in situ* measurements in a porcine carcass. Two experiments were conducted. The first mimicked the use of a body-worn receiving coil and showed that, like the high-frequency scheme, the best position for the receiving coil is near the location of the capsule. The second characterized the direction-dependent loss of the 32-MHz and 868-MHz transmission paths through the porcine carcass. Normalized to control measurements recorded in air, data from the second experiment emphasized the advantage of the near-field magnetically coupled 32-MHz scheme in two key areas. First, the tissue attenuation was only 1–5 dB on average at 32 MHz with no channel fading, but was 15–26 dB on average at 868 MHz with channel fading of up to 52 dB (corresponding to likely loss of data). We estimate the low-frequency capsule has better CSNR for similar levels of power consumption, in addition to having over 50 h of battery lifetime (four times the battery life of the 868-MHz scheme). Finally, we note that the performance advantages of the low-frequency scheme are coupled to a much smaller form factor, at one eighth of the volume of the 868-MHz scheme, allowing much greater miniaturization of future ingestible capsules, and, hence, increased patient comfort.

References

[1] G. Iddan, G. Meron, A. Glukhovsky, and P. Swain, "Wireless capsule endoscopy," *Nature*, vol. 405, p. 417, 2000.

[2] A. Alomainy, Y. Hao, X. Hu, C. G. Parini, and P. S. Hall, "UWB on-body radio propagation and system modelling for wireless body-centric networks," *Proc. IEE–Commun.*, vol. 153, no. 1, pp. 107–114, Feb. 2006.

[3] J. E. Pandolfino, J. E. Richter, T. Ours, J. M. Guardino, J. Chapman, and P. J. Kahrilas, "Ambulatory esophageal pH monitoring using a wireless system," *Amer. J. Gastroenterol.*, vol. 98, no. 4, pp. 740–749, 2003.

[4] A. Glukhovsky, "Wireless capsule endoscopy," *Sensor Rev.*, vol. 23, no. 2, pp. 128–133, 2003.

[5] V. K. Zworykin, "Radio pill," *Nature*, vol. 179, p. 898, 1957.

[6] R. S. Mackay, "Radio telemetering from within the body," *Science*, vol. 134, pp. 1196–1202, 1961.

[7] H. G. Noller, "Die Endoradiosonde. Zur elektronischen pH-messung im Magen und ihre klinische Bedeutung," *Deutsche Medizinische Wochenschrift*, vol. 85, p. 1707, 1960.

[8] K. Kramer and L. B. Kinter, "Evaluation and applications of radio telemetry in small laboratory animals," *Physiol. Genom.*, vol. 29, pp. 1035–1041, 1988.

[9] N. F. Timmons and W. G. Scanlon, "Analysis of the performance of IEEE 802.15.4 for medical sensor body area networking," in *Proc. 1st Annu. IEEE Commun. Soc. Conf. Sensor and Ad Hoc Commun. and Networks*, Santa Clara, CA, Oct. 2004, pp. 16–24.

[10] W. G. Scanlon, J. B. Burns, and N. E. Evans, "Radio wave propagation from a tissue-implanted source at 418 MHz and 916.5 MHz," *IEEE Trans. Biomed. Eng.*, vol. 47, no. 4, pp. 527–533, 2000.

[11] R. H. Colson, "A review of short range inductive loop telemetry system design," in *Proc. Workshop Alternative Methods for Radio Telemetry* (in German), Garmisch-Partenkirchen, Germany, May 1983, pp. 277–288.

[12] L. C. Chirwa, P. A. Hammond, S. Roy, and D. R. S. Cumming, "Electromagnetic radiation from ingested sources in the human intestine between 150 MHz and 1.2 GHz," *IEEE Trans. Biomed. Eng.*, vol. 50, no. 4, pp. 484–492, 2003.

[13] H. Adel, R. Wansch, and C. Schmidt, "Antennas for a body area network," in *Proc. IEEE Antennas Propagat. Soc. Int. Symp.*, Jun. 2003, vol. 1, pp. 471–474.

[14] E. Farella, A. Pieracci, D. Brunelli, L. Benini, B. Ricco, and A. Acquaviva, "Design and implementation of WiMoCA node for a body area wireless sensor network," in *Proc. IEEE Syst. Commun.*, Aug. 2005, pp. 342–347.

[15] J. Ryckaert, C. Desset, A. Fort, M. Badaroglu, V. De Heyn, P. Wambacq, G. Van der Plas, S. Donnay, B. Van Poucke, and B. Gyselinckx, "Ultra-wideband transmitter for low-power wireless body area networks: Design and evaluation," *IEEE Trans. Circuits Syst. I: Reg. Papers*, vol. 52, no. 12, pp. 2515–2525, Dec. 2005.

[16] K. Finkenzeller, *RFID Handbook: Fundamentals and Applications in Contactless Smart Cards and Identification*, 2nd ed. New York: Wiley, 2003, ch. 3.

[17] M. Ahmadian, B. W. Flynn, A. F. Murray, and D. R. S. Cumming, "Data transmission for implantable microsystems using magnetic coupling," *IEE Proc.–Commun.*, vol. 152, no. 2, pp. 247–250, Apr. 2005.

[18] *Radiocommunications Agency Short Range Devices Information Sheet*, RA-114, Rev 10, Mar. 2003 [Online]. Available: http://www.ofcom.org.uk/static/archive/ra/publication/ra_info/ra114.htm, accessed Apr. 10, 2006

[19] L. Wang, E. A. Johannessen, L. Cui, C. Ramsay, T. B. Tang, M. Ahamadian, A. Astaras, P. W. Dickman, J. M. Cooper, A. F. Murray, B. W. Flynn, S. P. Beaumont, and D. R. S. Cumming, "Networked wireless microsystem for remote gastrointestinal monitoring," in *Dig. Tech. Papers 12th Int. Conf. Transducers, Solid-State Sensors, Actuators Microsyst.*, Boston, MA, Jun. 2003, pp. 1184–1187.

[20] E. A. Johannessen, L. Wang, C. Wyse, D. R. S. Cumming, and J. M. Cooper, "Biocompatibility of a lab-on-a-pill sensor in artificial gastrointestinal environments," *IEEE Trans. Biomed. Eng.*, vol. 53, no. 11, pp. 2333–2340, Nov. 2006.

[21] Epcos B82498 datasheet Epcos, Munich, Germany, Apr. 10, 2006 [Online]. Available: http://www.epcos.com/inf/30/ds/b82498f.pdf

[22] L. Wang, E. Johannessen, P. Hammond, L. Cui, J. Cooper, S. Reid, and D. R. S. Cumming, "A programmable microsystem using system-on-chip for real-time biotelemetry," *IEEE Trans. Biomed. Eng.*, vol. 52, no. 7, pp. 1251–1260, Jul. 2005.

[23] J. Kraus, *Antennas*, 3rd ed. Boston, MA: McGraw-Hill, 2002.

[24] A. Taflove and S. C. Hagness, *Computational Electrodynamics*, 2nd ed. Boston, MA: Artech, 2000.

[25] S. Gabriely, R. W. Lau, and C. Gabriel, "The dielectric properties of biological tissues: III. Parametric models for the dielectric spectrum of tissues," *Phys. Med. Biol.*, vol. 41, pp. 2271–2293, 1996.

Lei Wang (M'03) received the B.Eng. degree in information and control engineering and the Ph.D. degree in biomedical engineering from the Xi'an Jiaotong University, Xi'an, China, in 1995 and 2000, respectively.

During 2000, he held a Henry Lester Postdoctoral Research Scholarship at the University of Dundee, Dundee, U.K. He joined the Microsystem Technology Research Group, Department of Electronics and Electrical Engineering, University of Glasgow, Glasgow, U.K., in 2001. Since then, he has primarily worked on an Integrated Diagnostics for Environmental and Analytical System project and a Laboratory-In-A-Pill Feasibility Study project. His research interests include integrated circuits and systems design, digital signal processing, and biomedical instrumentation.

Timothy D. Drysdale received the B.E. (1st Class Hons., University Prize) and Ph.D. degrees in electrical and electronic engineering from the University of Canterbury, Christchurch, New Zealand, in 1998 and 2003, respectively.

In 2006, he was appointed as a Lecturer in the Electronics Design Centre at the University of Glasgow, Glasgow, U.K., where he leads the Electromagnetics Design Group. He joined the Microsystem Technology Research Group, Department of Electronics and Electrical Engineering, University of Glasgow, in 2002. He has researched the design, modelling, and characterization of radio frequency and terahertz devices, leading to one patent and three patent applications. His current research interests also relate to electromagnetics aspects of electronics design.

Dr. Drysdale is a member of the Applied Computational Electromagnetics Society. He was awarded a Scottish Executive/Royal Society of Edinburgh Personal Research Fellowship in 2004.

David R. S. Cumming received the B.Eng. degree in electronics and electrical engineering from the University of Glasgow, Glasgow, U.K., and the Ph.D. degree in microelectronics and physics from Cambridge University, Cambridge, U.K., in 1989 and 1993, respectively.

He worked as a Silicon Design Engineer in U.K. industry before returning to research in nanotechnology at the University of Glasgow, where he became an 1851 Research Fellow. In 1997, he joined the staff of the University of Canterbury, Christchurch, New Zealand, before returning to the University of Glasgow to take up a similar position. He is now Professor of microsystem technology and Director of the Electronics Design Centre for Heterogeneous Systems at the University of Glasgow. His research is focused on integrated microsensor systems and instrumentation, and microfabrication for applications such as terahertz optics and nanodevices. Much of his work is at the interface between electronics and biomedical research, and he has recently become the co-founder of a university spin-out, Wireless Biodevices Ltd.